26th ABCM International Congress of Mechanical Engineering
November 22-26, 2021. Florianópolis, SC, Brazil

COB-2021-0084
Estimation of Shaft Speed and Load Inertia Applied to Induction Motor Using Kalman Filter for Unknown Inputs

Daniel de Lemos Santos
Thiago Pereira das Chagas
Gildson Queiroz de Jesus
Vinícius Souza Madureira
Matheus Garcia Soares
Departamento de Ciências Exatas e Tecnológicas, Universidade Estadual de Santa Cruz, Ilhéus-Bahia, Brasil.
dandelemos@gmail.com, tpchagas@uesc.br, gildsonj@gmail.com, vinicius.madu@gmail.com, mgsoares@uesc.br

Abstract. *The induction motors data acquisition is commonly made by using sensors which reduce the motor simplicity and are expensive. Based on this, using less intrusive sensors that can operate at higher sampling periods, such as current sensors and voltmeters, constitutes a suited solution. This paper presents a method for induction motors shaft speed and inertia estimation based on a modified Kalman filter for unknown inputs. A compatible nonlinear motor model was obtained and the load inertia was modeled as an unknown input. The results for the simulated case showed normalized root mean square error (nRMSE) of* 0.0006% *and* 0.0142% *for shaft speed and load inertia, respectively. The proposed methodology also estimates the stator and rotor currents (nRMSEs maximum of* 0.0219% *and* 0.076%*, respectively) and the motor torque (nRMSE of* 0.019%*). These estimates were computed based on the measurement of currents and voltages at stator terminals considering model and sensor noises and in the vicinity of the motor nominal operating point. Therefore, estimation based on the modified KFUI is a simpler and more cost-effective alternative for acquiring measurements from induction machines than sensors.*

Keywords: *induction motors, sensorless, torque estimation, currents estimation, filtering, optimization.*

1. INTRODUCTION

The three phase induction motors became very common because of their easy adaptability to different loads and the low costs in repairing and construction. They are by far the most widely used motor in the industry (Rashid, 2011), in applications such as pumps, steel mills and winch drives. Also, on a smaller scale, induction machines are used as the controlled drive motor in vehicles, air conditioning systems, and in wind turbines, for example (Krause et al., 2013).

A good measurement of motor operating data, especially shaft speed, torque and currents, allows to expand their uses into more sensitive and complex mechanical systems. However, this data extraction is commonly made by using sensors which are physically complicated to implement and more expensive as they are more accurate. Accordingly to Giri (2013), "complex instrumentation placed on an induction motor would only cancel the major strength of this device - simplicity". So, instead of a tachometer and inertial sensors, using current and voltage sensors to get motor data is a suited solution because they are cheaper, less intrusive and can operate at higher sampling periods. Besides that, the inertia on the motor shaft is a particularly characteristic value of the type of motor load (Mamede Filho, 2007) and directly affects motor operation. However, loads with high variability present inertia of unknown behavior that can reduce the reliability of the estimation of the motor operating point. Therefore, in the present work, the load inertia is treated as a variable, specifically, an unknown input.

In literature, some studies that use Kalman filtering as induction motor model-based estimator are Jayaramu et al. (2021), Stender et al. (2020), Zerdali and Barut (2018), Zerdali and Demir (2021), Alonge and D'Ippolito (2010). In Jayaramu et al. (2021) and Stender et al. (2020) the induction motor models used are based on infinite inertia hypothesis (Bolognani et al., 1999), which considers rotor speed dynamics negligible compared to other state variables. Also, Stender et al. (2020) focus on only steady-state torque measurements because it lacks information of the behavior of load machine and the total rotational inertia coupled at the motor shaft to obtain the exact dynamic operation of the test motor. Zerdali and Demir (2021), Zerdali and Barut (2018) and Alonge and D'Ippolito (2010) consider rotor speed to be a dynamic state using the equation of motion, but their estimation process ignores the effect of load and inertia changes on the state estimates.

The main contribution of this paper is to provide a methodology of three phase induction motor speed and load inertia estimation from its nominal operating point based on the proposition of a modification of Kalman filter for unknown inputs

(KFUI) (Darouach et al., 1995). This modified KFUI consists on a discrete-time low pass butterworth filter, adjusted by genetic algorithm, implemented into the original KFUI to improve its filtering capability and the precision of the unknown input estimation. KFUI uses a linear discrete state space system model and real-time measurement of outputs and inputs to estimate the state and the unknown inputs. A nonlinear induction motor model is used, which goes through linearization and discretization steps to obtain a system model compatible with the KFUI.

The advantage of this methodology is that it requires only voltage and current sensors on the stator terminals. These measured currents and the other state variables such as rotor currents and shaft speed, in addition to motor torque and load inertia, are estimated. Therefore, shaft speed and inertia estimation, using the modified KFUI, consists of a cheaper and precise alternative to sensors.

A simulation is carried out to illustrate the efficiency of the proposed methodology. The case study consists in motor operation considering supply voltage variations on the stator terminals, a generic load curve on the motor shaft and modeling and measurement uncertainties. Furthermore, the accuracy of the estimation for different levels of noises is presented using the same parameters as the case study.

The manuscript is divided as follows. The three-phase induction motor model is presented in Section 2. The KFUI and the proposed modification are presented in Section 3. The methodology for applying the modified KFUI to the non-linear motor model is presented in Section 4. Section 5 is dedicated to simulated results and Section 6 for final conclusions and future work.

2. INDUCTION MOTOR MODEL

This section presents the procedure to obtain a three phase induction motor state space model. This model is developed transferring a three phase symmetrical induction machine to a two phase synchronously rotating reference-frame of $dq0$ axis. This approach is done because the $dq0$ system preserves the original system's features with a reduction in the number of problem variables. Also, this transformation presents a change of variables that eliminates the position-dependent mutual inductances of a symmetrical induction machine (Krause et al., 2013). The correlation between these systems is made by using Eq. (1) and Eq. (2), where θ is the angle between abc and $dq0$ axes, $f_{a,b,c}$ and $f_{d,q,0}$ are generic variables (Krause et al., 2013).

$$\begin{bmatrix} f_d \\ f_q \\ f_0 \end{bmatrix} = \frac{2}{3} \begin{bmatrix} \cos\theta & \cos(\theta - \frac{2\pi}{3}) & \cos(\theta + \frac{2\pi}{3}) \\ \sin\theta & \sin(\theta - \frac{2\pi}{3}) & \sin(\theta + \frac{2\pi}{3}) \\ \frac{1}{2} & \frac{1}{2} & \frac{1}{2} \end{bmatrix} \begin{bmatrix} f_a \\ f_b \\ f_c \end{bmatrix} \tag{1}$$

$$\begin{bmatrix} f_a \\ f_b \\ f_c \end{bmatrix} = \begin{bmatrix} \cos\theta & \sin\theta & 1 \\ \cos(\theta - \frac{2\pi}{3}) & \sin(\theta - \frac{2\pi}{3}) & 1 \\ \cos(\theta + \frac{2\pi}{3}) & \sin(\theta + \frac{2\pi}{3}) & 1 \end{bmatrix} \begin{bmatrix} f_d \\ f_q \\ f_0 \end{bmatrix} \tag{2}$$

Using Ohm's and Faraday's laws, it's obtained the voltage equations of induction machine (Krause et al., 2013). They are rewritten to flux linkage equations in the state space form in Eq. (3) to Eq. (6) in terms of the voltage.

$$\dot{\lambda}_{qs}(t) = \omega_b \, v_{qs}(t) - \omega_b \, r_s \, i_{qs}(t) - \omega \lambda_{ds}(t) \tag{3}$$

$$\dot{\lambda}_{ds}(t) = \omega_b \, v_{ds}(t) - \omega_b \, r_s \, i_{ds}(t) + \omega \lambda_{qs}(t) \tag{4}$$

$$\dot{\lambda}_{qr}(t) = \omega_b \, v_{qr'}(t) - \omega_b \, r_{r'} \, i_{qr'}(t) - (\omega - \omega_r(t)) \lambda_{dr}(t) \tag{5}$$

$$\dot{\lambda}_{dr}(t) = \omega_b \, v_{dr'}(t) - \omega_b \, r_{r'} \, i_{dr'}(t) + (\omega - \omega_r(t)) \lambda_{qr}(t) \tag{6}$$

Which $i_{d,q}$ represents currents, $v_{d,q}$ represents voltages, $\lambda_{d,q}$ represents the flux linkages and ω_r is the rotor angular speed. The subscripts s and r refer to stator and rotor, respectively. The subscript r' refer to rotor electrical quantities referred to stator side. So, r_s and $r_{r'}$ are the stator and rotor electrical resistances, respectively. ω_b is the base electrical angular speed used to calculate the impedances. Rotor voltages $v_{qr'}$ and $v_{dr'}$ are zero because the rotor conductors are shorted.

In order to transform the system's electric equations given by Eq. (3) to Eq. (6) into a model described by currents equations, it's assumed the magnetic circuit is linear. This assumption consider that the entire magnetic flux of the machine is contained in the air gap. Accordingly to Krause et al. (2013), in the majority of applications, the motor behavior can be adequately predicted using this simplified representation. It fits better specially in high performance motor models. So, the flux linkages are related to currents by the equations Eq. (7) to Eq. (10) (Krause et al., 2013),

$$\lambda_{qs}(t) = L_{ls} i_{qs}(t) + M(i_{qs}(t) + i_{qr'}(t)) \tag{7}$$

$$\lambda_{ds}(t) = L_{ls} i_{ds}(t) + M(i_{ds}(t) + i_{dr'}(t)) \tag{8}$$

$$\lambda_{qr}(t) = L_{lr'} i_{qr'}(t) + M(i_{qs}(t) + i_{qr'}(t)) \tag{9}$$

$$\lambda_{dr}(t) = L_{lr'} i_{dr'}(t) + M(i_{ds}(t) + i_{dr'}(t)) \tag{10}$$

with

$$M = \frac{3}{2} L_m \tag{11}$$

Where L_{ls} and $L_{lr'}$ are the stator and rotor leakage inductances, respectively. L_m is the magnetic inductance. The Eq. (7) to Eq. (10) were applied in Eq. (3) to Eq. (6). Thus, the system's electric differential equations, Eq. (12) to Eq. (15), are expressed in terms of currents as

$$\dot{i}_{qs} = \Delta \left[(X_{lr'} + X_M) v_{qs} - \frac{\omega X_Z + X_M^2 \omega_r}{\omega_b} i_{ds} - \frac{X_M (X_{lr'} + X_M) \omega_r}{\omega_b} i_{dr'} + Z_1 \, i_{qs} + Z_2 \, i_{qr'} \right] \tag{12}$$

$$\dot{i}_{ds} = \Delta \left[(X_{lr'} + X_M) v_{ds} + \frac{\omega X_Z + X_M^2 \omega_r}{\omega_b} i_{qs} + \frac{X_M (X_{lr'} + X_M) \omega_r}{\omega_b} i_{qr'} + Z_3 \, i_{ds} + Z_4 \, i_{dr'} \right] \tag{13}$$

$$\dot{i}_{qr'} = \Delta \left[-X_M v_{qs} - \frac{(\omega - \omega_r) X_Z - X_M^2 \omega_r}{\omega_b} i_{dr'} + \frac{X_M (X_{ls} + X_M) \omega_r}{\omega_b} i_{ds} - Z_5 \, i_{qr'} - Z_6 \, i_{qs} \right] \tag{14}$$

$$\dot{i}_{dr'} = \Delta \left[-X_M v_{ds} + \frac{(\omega - \omega_r) X_Z - X_M^2 \omega_r}{\omega_b} i_{qr'} - \frac{X_M (X_{ls} + X_M) \omega_r}{\omega_b} i_{qs} - Z_7 \, i_{dr'} - Z_8 \, i_{ds} \right] \tag{15}$$

with,

$$X_Z = X_{lr'} X_{ls} + X_M (X_{lr'} + X_{ls}) \tag{16}$$

$$Z_1 = \left[\frac{X_{S_1} (X_{ls} + X_M)}{X_{ls}} + \frac{X_{S_2} X_M}{X_{lr'}} \right] \tag{17}$$

$$Z_2 = \left[\frac{X_{S_1} X_M}{X_{ls}} + \frac{X_{S_2} (X_{lr'} + X_M)}{X_{lr'}} \right] \tag{18}$$

$$Z_3 = \left[\frac{X_{S_1} (X_{ls} + X_M)}{X_{ls}} + \frac{X_{S_3} X_M}{X_{lr'}} \right] \tag{19}$$

$$Z_4 = \left[\frac{X_{S_1} X_M}{X_{ls}} + \frac{X_{S_3} (X_{lr'} + X_M)}{X_{lr'}} \right] \tag{20}$$

$$Z_5 = \left[\frac{X_{R_1} (X_{lr'} + X_M)}{X_{lr}} + \frac{X_{R_3} X_M}{X_{ls}} \right] \tag{21}$$

$$Z_6 = \left[\frac{X_{R_1} X_M}{X_{lr}} + \frac{X_{R_3} (X_{ls} + X_M)}{X_{ls}} \right] \tag{22}$$

$$Z_7 = \left[\frac{X_{R_2} (X_{lr'} + X_M)}{X_{lr}} + \frac{X_{R_3} X_M}{X_{ls}} \right] \tag{23}$$

$$Z_8 = \left[\frac{X_{R_2} X_M}{X_{lr}} + \frac{X_{R_3} (X_{ls} + X_M)}{X_{ls}} \right] \tag{24}$$

$$X_{S_1} = \left[\frac{r_s (X_{ml} - X_{ls})(X_{lr'} + X_M)}{X_{ls}} - \frac{r_{r'} X_{ml} X_M}{X_{lr'}} \right] \tag{25}$$

$$X_{S_2} = \left[\frac{r_s X_{ml} (X_{lr'} + X_M)}{X_{ls}} - \frac{r_{r'} X_M (X_{ml} - X_{lr'})}{X_{lr'}} \right] \tag{26}$$

$$X_{S_3} = \left[\frac{r_s X_{ml} (X_{lr'} + X_M)}{X_{ls}} + \frac{r_{r'} X_M (X_{ml} - X_{lr'})}{X_{lr'}} \right] \tag{27}$$

$$X_{R_1} = \left[\frac{r_s X_{ml} X_M}{X_{ls}} - \frac{r_{r'} (X_{ml} - X_{lr'})(X_{ls} + X_M)}{X_{lr'}} \right] \tag{28}$$

$$X_{R_2} = \left[\frac{r_s X_{ml} X_M}{X_{ls}} + \frac{r_{r'} (X_{ml} + X_{lr'})(X_{ls} + X_M)}{X_{lr'}} \right] \tag{29}$$

$$X_{R_3} = \left[\frac{r_s (X_{ml} - X_{ls}) X_M}{X_{ls}} - \frac{r_{r'} X_{ml} (X_{ls} + X_M)}{X_{lr'}} \right] \tag{30}$$

$$\Delta = \frac{\omega_b}{(X_{lr'}L_{ls} + X_M X_{ls} + X_M X_{lr'})} \tag{31}$$

$$X_{ml} = \left(\frac{1}{X_{ls}} + \frac{1}{X_{lr'}} + \frac{1}{X_{Lm}}\right)^{-1} \tag{32}$$

considering X_{ls} ,$X_{lr'}$,X_{Lm} and X_M as the reactances corresponding to the inductances of Eq. (7) to Eq. (11).

Using the Principle of Moments (Halliday et al., 1996), the angular speed equation is obtained and described by Eq. (33),

$$\dot{\omega}_r(t) = \frac{P}{2(J_m + J_L(t))}\left[T_e(t) - (k_a\,\omega_r^2 + k_v\,\omega_r + T_L(t))\right] \tag{33}$$

with

$$T_e(t) = \frac{3PX_M}{4\,\omega_b}(i_{qs}(t)\,i_{dr'}(t) - i_{ds}(t)\,i_{qr'}(t)) \tag{34}$$

$$T_L(t) = \frac{T_N}{J_N}J_L(t) \tag{35}$$

where k_a and k_v are, respectively, the friction coefficient of air and oil viscosity and P is number of poles. J_m and J_L are the rotor and load inertias, the last one is possibly variable in the present work. T_e and T_L are the electromagnetic and load torques, respectively. T_N is the nominal torque and J_N is the nominal load inertia, they are obtained from motor nameplate and modeling tests, respectively.

Therefore, the motor model is unified and described by Eq. (36) and Eq. (37).

$$\frac{d\,x(t)}{dt} = f(x(t), u(t), d(t)) \tag{36}$$

$$y(t) = g(x(t), u(t), d(t)); \tag{37}$$

Where $x(t) = \begin{bmatrix} i_{qs}(t) & i_{ds}(t) & i_{qr'}(t) & i_{dr'}(t) & \omega_r(t) \end{bmatrix}^T$ is the state vector, $u(t) = \begin{bmatrix} v_{qs}(t) & v_{ds}(t) \end{bmatrix}^T$ is the control vector and $d = J_L(t)$ is the variable treated as the system's unknown input. f is the function composed of Eq. (12) to Eq. (15) and Eq. (33). g is the measurement function which gathers the objective state variables measures at the output vector y. In this work, $y(t) = \begin{bmatrix} i_{qs}(t) & i_{ds}(t) \end{bmatrix}$.

3. MODIFIED KALMAN FILTER FOR UNKNOWN INPUTS

The KFUI is presented in this section following Darouach et al. (1995). Next, its weakness for the proposed application is highlighted and an alternative to overcome it is formulated as one of the contributions of this article.

Consider the invariant and discrete-time state space system shown in Eq. (38) and Eq. (39),

$$\mathbf{x}_{k+1} = \mathbf{A}\,\mathbf{x}_k + \mathbf{B}\,\mathbf{u}_k + \mathbf{F}\,\mathbf{d}_k + \mathbf{w}_k \tag{38}$$

$$\mathbf{y}_{k+1} = \mathbf{H}\,\mathbf{x}_{k+1} + \mathbf{v}_k \tag{39}$$

in which the state vector is $\mathbf{x}_k \in \mathbb{R}^n$; the control input vector is $\mathbf{u}_k \in \mathbb{R}^m$; $\mathbf{d}_k \in \mathbb{R}^q$ is the unknown input vector; $\mathbf{y}_{k+1} \in \mathbb{R}^p$ is the output vector; $\mathbf{A} \in \mathbb{R}^{n\times n}$ is the system parameter matrix. $\mathbf{B} \in \mathbb{R}^{n\times m}$ is the control parameter matrix; $\mathbf{F} \in \mathbb{R}^{n\times q}$ is the unknown input parameter matrix; $\mathbf{H} \in \mathbb{R}^{p\times n}$ is the output parameter matrix; $\mathbf{v}_k \in \mathbb{R}^p$ and $\mathbf{w}_k \in \mathbb{R}^n$ are zero mean gaussian white noise vectors uncorrelated to each other and to the system's initial state, with covariates $\mathbf{V} \in \mathbb{R}^{p\times p}$ and $\mathbf{W} \in \mathbb{R}^{n\times n}$, respectively; and k denotes an integer time index from 0 to $N-1$ for N available measures.

Then, the optimal unknown input and state estimates, respectively $\widehat{\mathbf{d}}$ and $\widehat{\mathbf{x}}$, are given by Eq. (40) to Eq. (42),

$$\overline{\mathbf{x}}_{k|k} = \mathbf{A}\,\widehat{\mathbf{x}}_{k|k} + \mathbf{B}\,\mathbf{u}_k \tag{40}$$

$$\widehat{\mathbf{d}}_{k|k+1} = \mathbf{K}^d_{k+1}(\mathbf{y}_{k+1} - \mathbf{H}\,\overline{\mathbf{x}}_{k|k}) \tag{41}$$

$$\widehat{\mathbf{x}}_{k+1|k+1} = \overline{\mathbf{x}}_{k|k} + \mathbf{F}\,\widehat{\mathbf{d}}_{k|k+1} + \mathbf{K}^x_{k+1}(\mathbf{y}_{k+1} - \mathbf{H}(\overline{\mathbf{x}}_{k|k} + \mathbf{F}\,\widehat{\mathbf{d}}_{k|k+1})) \tag{42}$$

where $\mathbf{K}^x_{k+1}$ and $\mathbf{K}^d_{k+1}$ are the Kalman gains for the state and unknown input, respectively. They are computed using Eq. (43) and Eq. (44),

$$\mathbf{K}^x_{k+1} = (\overline{\mathbf{P}}^{-1}_{k|k} + \mathbf{H}^T\mathbf{V}^{-1}\mathbf{H})^{-1}\mathbf{H}^T\mathbf{V}^{-1} \tag{43}$$

$$\mathbf{K}^d_{k+1} = \mathbf{P}^{dx}_{k+1|k+1}\mathbf{H}^T\mathbf{V}^{-1} \tag{44}$$

with

$$\overline{\mathbf{P}}_{k|k} = \mathbf{A}\mathbf{P}^x_{k|k}\mathbf{A}^T + \mathbf{W} \tag{45}$$

$$\mathbf{P}^d_{k|k+1} = (\mathbf{F}^T\mathbf{H}^T(\mathbf{V} + \mathbf{H}\,\overline{\mathbf{P}}_{k|k}\mathbf{H}^T)^{-1}\mathbf{H}\mathbf{F})^{-1} \tag{46}$$

$$\mathbf{P}^{xd}_{k+1|k+1} = \mathbf{P}^x_{k+1|k+1}\overline{\mathbf{P}}^{-1}_{k|k}\mathbf{F}\,(\mathbf{F}^T\,\overline{\mathbf{P}}^{-1}_{k|k}\mathbf{F})^{-1} \tag{47}$$

$$\mathbf{P}^x_{k+1|k+1} = (\overline{\mathbf{P}}^{-1}_{k|k} + \mathbf{H}^T\mathbf{V}^{-1}\mathbf{H} - \overline{\mathbf{P}}^{-1}_{k|k}\mathbf{F}(\mathbf{F}^T\,\overline{\mathbf{P}}^{-1}_{k|k}\mathbf{F})^{-1}\mathbf{F}^T\,\overline{\mathbf{P}}^{-1}_{k|k})^{-1} \tag{48}$$

$\mathbf{P}^x \in \mathbb{R}^{n\times n}$ is the state estimation error covariance matrix with size, $\mathbf{P}^d \in \mathbb{R}^{q\times q}$ is the unknown input estimation covariance matrix and $\mathbf{P}^{xd} \in \mathbb{R}^{q\times n}$ is the cross state and unknown input estimation error covariance matrix with $\mathbf{P}^{dx} = (\mathbf{P}^{xd})^T$.

The KFUI's covariance matrices $\mathbf{W}$, $\mathbf{V}$ and initial $\mathbf{P}^x_{k|k}$ must be designed based on model and measurement reliability.

Remark. *The KFUI formulation does not filter state and measurement noises propagated to the unknown input estimate. The results of the original KFUI application showed high noises for the load inertia estimates*[1] *and the same problem was faced by Madureira et al. (2020).*

So, a first order discrete-time low-pass Butterworth filter (LPBF) was used to improve the KFUI filtering capability and precision of the unknown input estimation. The LPBF's transfer function $D(z)$ is shown in Eq. (49) (Oppenheim et al., 1996).

$$D(z) = \frac{h_1 + h_2\,z^{-1}}{g_1 + g_2\,z^{-1}} \tag{49}$$

Where g and h are the numerator and denominator coefficients of the LPBF Z transfer function, respectively. Therefore, consider the following Proposition:

Proposition 1. *Given the first order discrete-time LPBF Z transfer function Eq. (49), unknown input estimate noise is filtered by applying the inverse Z transform of Eq. (49) to Eq. (41) resulting in Eq. (50). KFUI is applied using Eq. (50) in place of Eq. (41).*

$$\hat{\mathbf{d}}_{k|k+1} = -\frac{g_2}{g_1}\hat{\mathbf{d}}_{k-1|k} + \frac{h_1}{g_1}\mathbf{K}^d_{k+1}(\mathbf{y}_{k+1} - \mathbf{H}\overline{\mathbf{x}}_{k|k}) + \frac{h_2}{g_1}\mathbf{K}^d_k(\mathbf{y}_k - \mathbf{H}\overline{\mathbf{x}}_{k|k}) \tag{50}$$

Proof.

$$\mathcal{Z}^{-1}[O(z)] = \mathcal{Z}^{-1}[D(z)L(z)] \;\therefore\; o_k = -\frac{g_2}{g_1}o_{k-1} + \frac{h_1}{g_1}l_k + \frac{h_2}{g_1}l_{k-1} \tag{51}$$

Where $O(z)$ and $L(z)$ are the Z transforms of LPBF's output o and input l, respectively. Considering l_k equal to Eq. (41) and $o_k = \hat{\mathbf{d}}_{k|k+1}$ in Eq. (51), the Eq. (50) is obtained. □

Finally, the LPBF's parameters are designed according to the system and external features.

4. METHODOLOGICAL APPLICATION

This section presents the steps to obtain the motor model in a form compatible with the modified KFUI and how to apply it. Also, it shows the procedure to design the filter's parameters.

4.1 Linearization and discretization

The modified KFUI is applicable to linear and discrete-time state space models. However, the obtained motor model is nonlinear and continuous time. Therefore, the linearization and discretization processes are carried out and explained in this subsection.

Truncated Taylor series linearization is used. Given the motor model described by Eq. (36) and Eq. (37), the approximation at the operating point (x_o, u_o, d_o) and at the output y are calculated by Eq. (52) and Eq. (53).

$$\frac{d\,x(t)}{dt} \approx f(x_o, u_o, d_o) + \mathcal{A}\,\tilde{x}(t) + \mathcal{B}\,\tilde{u}(t) + \mathcal{F}\,\tilde{d}(t) \tag{52}$$

[1] These results are omitted in the present manuscript.

$$y(t) \approx g(x_o, u_o, d_o) + \mathcal{H}\,\tilde{x}(t) \tag{53}$$

Where $\tilde{x}$, $\tilde{u}$ and $\tilde{d}$ are small variation around x_o, u_o, d_o. Also,

$$\mathcal{A} = \frac{d\,f(x,u,d)}{dx}\Big|_{x=x_o,u=u_o,d=d_o}, \qquad \mathcal{B} = \frac{d\,f(x,u,d)}{du}\Big|_{x=x_o,u=u_o,d=d_o},$$

$$\mathcal{F} = \frac{d\,f(x,u,d)}{d\,d}\Big|_{x=x_o,u=u_o,d=d_o}, \qquad \mathcal{H} = \frac{d\,g(x,u,d)}{dx}\Big|_{x=x_o,u=u_o,d=d_o}.$$

The small variation linear system dynamics is presented by Eq. (54) and Eq. (55).

$$\frac{d\,\tilde{x}(t)}{dt} = \mathcal{A}\,\tilde{x}(t) + \mathcal{B}\,\tilde{u}(t) + \mathcal{F}\,\tilde{d}(t) \tag{54}$$

$$\tilde{y}(t) = \mathcal{H}\,\tilde{x}(t) \tag{55}$$

Relation between nonlinear and linearized variables are given by $x(t) \approx x_o + \tilde{x}(t)$, $u(t) \approx u_o + \tilde{u}(t)$, $d(t) \approx d_o + \tilde{d}(t)$ and $y(t) \approx y_o + \tilde{y}(t)$.

Applying this technique, the matrices $\mathcal{A}$, $\mathcal{B}$, $\mathcal{F}$ and $\mathcal{H}$ are obtained by substituting the quiescent operating point vectors $u_o = \begin{bmatrix} V_{qs} & V_{ds} \end{bmatrix}^T$, $d_o = J_{Lo}$ and $x_o = \begin{bmatrix} I_{qs} & I_{ds} & I_{qr'} & I_{dr'} & \Omega_r \end{bmatrix}^T$.

Finally, the discretization is done by the transformations below.

$$\mathcal{A} \to \mathbf{A},\ \mathcal{B} \to \mathbf{B},\ \mathcal{F} \to \mathbf{F},\ \mathcal{H} \to \mathbf{H}$$

$$x(t) \to \mathbf{x}_k, \tilde{x}(t) \to \tilde{\mathbf{x}}_k$$
$$u(t) \to \mathbf{u}_k, \tilde{u}(t) \to \tilde{\mathbf{u}}_k$$
$$d(t) \to \mathbf{d}_k, \tilde{d}(t) \to \tilde{\mathbf{d}}_k$$
$$y(t) \to \mathbf{y}_k, \tilde{y}(t) \to \tilde{\mathbf{y}}_k$$

This process was performed numerically on MATLAB software using the function *c2d*[2], which uses the state transition matrix and a zero-order holder to convert the continuous-time to discrete-time system with constant sample time. Before its using, $\mathcal{B}$ and $\mathcal{F}$ must be concatenated into an unique matrix $\begin{bmatrix} \mathcal{B} & \mathcal{F} \end{bmatrix}$, which is the system's global input jacobian matrix. After, $\mathbf{B}$ and $\mathbf{F}$ are restored from the obtained matrix.

Therefore, the resulting discrete-time linearized state space system compatible with the modified KFUI is shown in Eq. (56) and Eq. (57).

$$\tilde{\mathbf{x}}_{k+1} = \mathbf{A}\tilde{\mathbf{x}}_k + \mathbf{B}\tilde{\mathbf{u}}_k + \mathbf{F}\tilde{\mathbf{d}}_k \tag{56}$$

$$\tilde{\mathbf{y}}_k = \mathbf{H}\tilde{\mathbf{x}}_k \tag{57}$$

4.2 Applying the Modified KFUI in the discrete-time linearized model

This subsection explains the procedure to apply the modified KFUI into the obtained discrete-time linearized motor model and how to get the currents measurements from the nonlinear model.

Motor currents noisy measures, here obtained by simulation of the nonlinear noisy model, are used at the modified KFUI. It is done by summing gaussian white noises at the motor equations and the currents measurement. Both uncertainties attend to specific standard deviation based on the reliability of the model and the sensors considered.

Sensors measure the currents in abc form. So, to make this project approach more realistic and also able to apply the modified KFUI, the following procedure is done: first, the current dqo state variables gathered by $\mathcal{H}$ are transformed into the abc form; second, the gaussian white noises are added into this abc data to represent real sensor noise; then, the noisy abc state measures are transformed back into the dqo form and constitutes the actual measurement of motor currents used in the modified KFUI. The transformations used are shown in Eq. (1) and Eq. (2).

Figure 1 presents a block diagram that briefly illustrates how the methodology works. The real application can be implemented by replacing the "motor simulation" block with the real motor, where noisy current measurements are made directly by sensors at the stator terminals.

Once the parameters matrices $\mathbf{A}$, $\mathbf{B}$ and $\mathbf{F}$ are set, the state $\hat{\tilde{\mathbf{x}}}$ and unknown input $\hat{\tilde{\mathbf{d}}}$ estimates can be obtained for a given input $\tilde{\mathbf{u}}_k = \mathbf{u}_k - u_o$. Thus, $\hat{\mathbf{x}}$ and $\hat{\mathbf{d}}$ are calculated from Eq. (58) and Eq. (59), respectively.

$$\hat{\mathbf{x}}_k = x_o + \hat{\tilde{\mathbf{x}}}_k \tag{58}$$

$$\hat{\mathbf{d}}_k = d_o + \hat{\tilde{\mathbf{d}}}_k \tag{59}$$

[2]All MATLAB functions used in this manuscript are explained at https://www.mathworks.com/help/.

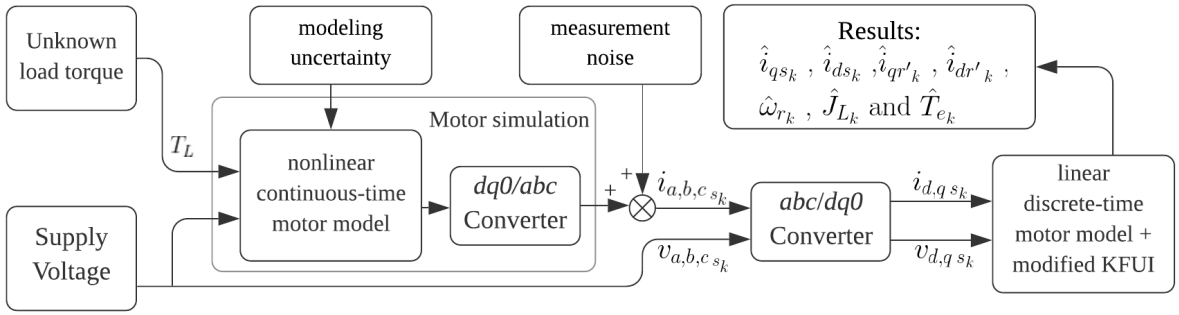

Figure 1. Block diagram of simulation

4.3 Optimization of modified KFUI parameters

This subsection is committed to explain the design of the modified KFUI parameters. This work performs the optimization on MATLAB software using Genetic Algorithm.

The LPBF's coefficients were defined by the function *butter* given a filter cut-off frequency f_c. The f_c and the KFUI's covariance matrices $\mathbf{W}$, $\mathbf{V}$ and initial $\mathbf{P}^x_{k|k}$ are optimized by using the function *ga*. The unknown input (load inertia) Root Mean Square Error was chosen as the objective function to be minimized.

The Genetic Algorithm requires examples to optimize the filter parameters, in particular the $u(t)$ and $d(t)$ curves for the motor simulation. These curves must be defined according to the specific requirements of the application in order to obtain suitable parameters.

This methodology estimates speed, inertia and torque at the motor shaft, as well the stator and rotor currents, from the measurement of the model voltages and stator currents. This arrangement is compatible with the real time data extraction from voltmeters and current sensors on a real three phase induction motor.

5. RESULTS

In this section, a case study of the presented methodology is carried out to exemplify its efficiency. The supply voltage and the load inertia small variations are applied to the motor model considering the state and measurement noises, and the load inertia, rotor speed and other state variables are estimated.

The results presented in the following are simulations using the three phase motor model presented in Section 2 with parameters set using WEG high efficiency Plus 1.5 HP 4P 220-380V motor nameplate and laboratory tests with values presented in Tab. 1. The quiescent operating point was selected to be the same of the nominal operation with supply voltage equal to 220 V and they are presented in Tab. 2.

Table 1. Motor's parameters and model specifications

Parameters	**Values**		
Motor power, kW	1.1	Magnetizing reactance, Ω	85.440
Frequency, Hz	60	Stator leakage reactance, Ω	6.410
Supply voltage, V	220	Rotor leakage reactance, Ω	6.414
Nominal current, A	2.56	Rotor resistance, Ω	5.058
Poles	4	Stator resistance, Ω	6.333
Nominal speed, rad/s	179.59	Base speed, rad/s	60π
Rotor inertia, kg.m^2	0.00328	Synchronous speed, rad/s	60π
Nominal load inertia, kg.m^2	0.060	Air friction coefficient	76μ
		Viscous friction coefficient	4μ

In order to reach reasonable results for more diverse operating situations, this approach was implemented considering a generic type of load variation in the motor shaft. This variation mixes steps, polynomials and exponential load curves, as shown in Fig. 4. However, the adjustments done by optimization can be made to set a better filtering operation to any type of target motor's load. Besides that, modeling and measurement uncertainties were considered at the simulation. They were included in the motor model and currents measures by adding gaussian white noises in Eq. (36) and Eq. (37). Their selected standard deviation are 0.1 and 0.05, respectively. These values are concatenated into the vector $\sigma = \begin{bmatrix}0.1 & 0.05\end{bmatrix}$. Based on this, the optimized values of LPBF's cut-off frequency and KFUI's covariance matrices are $f_c = 0.6107$ Hz,

Table 2. Quiescent operating points

Variables	Values
Quadrature stator current, A	-2.76
Direct stator current, A	2.00
Quadrature rotor current, A	0.57
Direct rotor current, A	-1.94
Rotor speed, rad/s	179.57
Load inertia, kg.m^2	0.06

$\mathbf{W} = 30.7857 \cdot \mathbf{I}_5$, $\mathbf{V} = 2.1081 \cdot \mathbf{I}_2$ and $\mathbf{P}_1^x = 35.1534 \cdot \mathbf{I}_5$, respectively. $\mathbf{I}_n$ are identity matrices of dimension n. Also, the LPBF's coefficients are $h_1 = h_2 = 0.0008$, $g_1 = 1$ and $g_2 = -0.9984$ for a sampling rate of 1.2 kHz. Figure 2 presents the voltage variations considered on the stator terminals. Normalized Mean Square Error (nRMSE) is used for simulation performance evaluation.

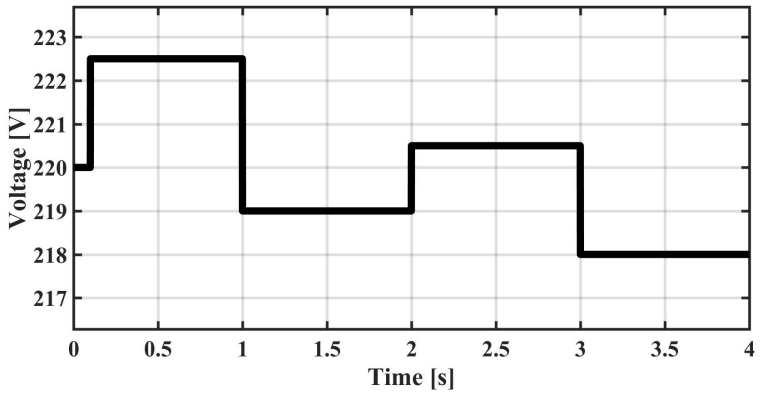

Figure 2. Supply voltage variations

The case study was carried out for σ and the curves resulting from the motor speed and load inertia estimates are presented in Fig. 3 and Fig. 4, respectively. From Fig. 3, the rotor speed estimates are very close of the actual values and their percentage errors lie below 0.2%. This indicates that the equation of motion of the model presents in its results less influence of noise and adopted uncertainties and provides a good approximation of the actual dynamics of the rotor speed with the aid of the modified KFUI. Accordingly to Fig. 4, the highest amount of error at the simulation is around the step change of the inertia curve and consists of a peak value around 8.00%. This happened because the adjustments made on LPBF's cut-off frequency are based on a generic approach applicable to any type of target load. Optimization can be executed to reduce erros in discontinuous variations in cases where several steps are expected. Nevertheless, for the remainder of inertia estimates in Fig. 4, the percentage errors are below 3.8%. These values also show the effectiveness of the proposed modification of the KFUI, since it considerably mitigates not only the influences of measurement noise and modeling uncertainty, but also the estimation errors of the state variables.

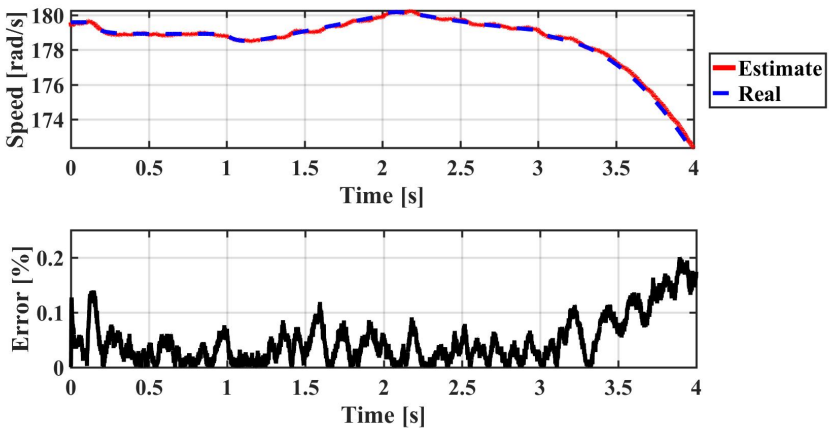

Figure 3. Motor speed estimation for σ

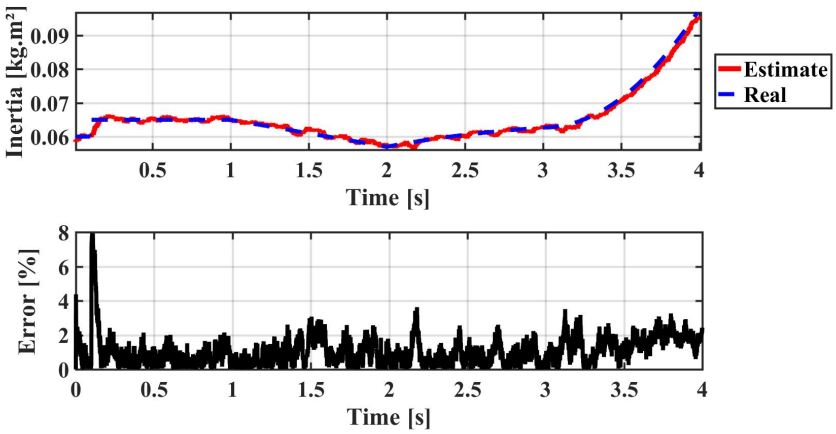

Figure 4. Inertia estimation for σ

The resulting nRMSEs for estimates of all state, load inertia, and motor torque variables are shown in the Tab. 3. The motor torque is computed by Eq. (34). Also, using the same parameters of the case study, Tab. 3 presents the estimation accuracy for different values of σ, which depends on the modeling and sensors reliability. The obtained nRMSEs for σ has an average value of 0.024% and a maximum of 0.076%. Considering a less reliable condition of 10σ, the average of nRMSEs is 0.216% and a maximum of 0.7129%. Best estimates, in general, occurred for the rotor speed and inertia, regardless of the adopted noise. This reinforces the good quality of rotor speed estimation by the proposed methodology and its ability to predict the load behavior.

Table 3. Case 2 estimates's nRMSE: Accuracy comparison for optimized versions using different standard deviation groups for modeling and measurement

nRMSE [%]				
Variables	0.5σ	σ	2σ	10σ
Quadrature stator current	0.0082	0.0165	0.0335	0.1588
Direct stator current	0.0108	0.0219	0.0390	0.1982
Quadrature rotor current	0.0381	0.0760	0.1375	0.7129
Direct rotor current	0.0106	0.0215	0.0384	0.1941
Rotor speed	0.0004	0.0006	0.0009	0.0039
Load inertia	0.0117	0.0142	0.0201	0.0725
Motor torque	0.0091	0.0190	0.0335	0.1717

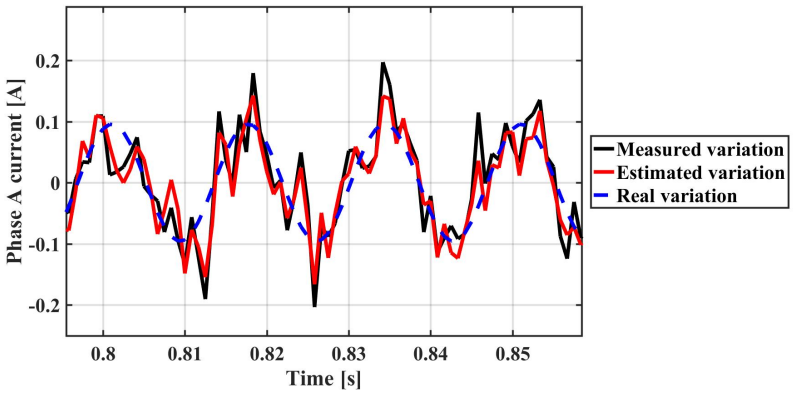

Figure 5. Comparison of measured, estimated, and actual variations of phase A current for σ in a simulation time window

Real, measured and estimated phase A currents are presented in Fig. 5 in order to exemplify the influence of noises with σ standard deviation on measurement. It presents the filtering effect on the estimates for the same time window and indicates the improvement in stator current measurements. This guarantees the usefulness of this methodology also to applications that have less accurate sensors.

6. CONCLUSION

In this paper, a methodology of shaft speed and inertia estimation was presented. To that end, a modified Kalman filter for unknown inputs (KFUI) and a mathematical model of an induction motor were used. The modified KFUI is obtained from the proposition of including a first order discrete-time low-pass Butterworth filter into the KFUI's unknown input equation. From the motor model, a state space system compatible with the KFUI is obtained, where the load inertia is considered an unknown input. A case study was carried out based on the motor operation under small variations in the supply voltage and a generalist load curve. An optimization was performed to achieve better results for estimates of the modified KFUI considering these operating conditions and specific modeling uncertainties and noise in the motor current measurements.

The results for shaft speed showed good estimation accuracy with percentage error below 0.2%. They also pointed out the robustness of the methodology against modeling uncertainties and noisy current measures by presenting maximum nRMSE of 0.0038% in the worst simulated condition. The results for the load inertia illustrated the improvement in the unknown input estimates by the modified KFUI proposition and its ability to predict the load behavior with a maximum nRMSE of 0.0725%. Furthermore, they highlighted the need to perform a specific optimization for the target load characteristic. This methodology also estimates the stator and rotor currents besides motor torque. For the higher adopted standard deviation of uncertainty and noise, the simulation showed nRMSEs of 0.1717% for the motor torque estimates and maximum nRMSEs of 0.1982% and 0.7129% for the stator and rotor currents, respectively.

Therefore, using the modified KFUI to acquire indution motors measures, such as the shaft speed, load inertia and torque, consists of a low cost and accurate alternative to sensors. In future works, this methodology will be applied to improve speed control performance and also using the extended Kalman filter methodology for operations outside the nominal point.

7. REFERENCES

F. Alonge and F. D'Ippolito. Robustness analysis of an extended kalman filter for sensorless control of induction motors. In *2010 IEEE International Symposium on Industrial Electronics*, pages 3257–3263. IEEE, 2010.

S. Bolognani, R. Oboe, and M. Zigliotto. Sensorless full-digital pmsm drive with ekf estimation of speed and rotor position. *IEEE transactions on Industrial Electronics*, 46(1):184–191, 1999.

M. Darouach, M. Zasadzinski, A. B. Onana, and S. Nowakowski. Kalman filtering with unknown inputs via optimal state estimation of singular systems. *International journal of systems science*, 26(10):2015–2028, 1995.

F. Giri. *AC electric motors control: advanced design techniques and applications*. John Wiley & Sons, 2013.

D. Halliday, R. Resnick, and J. Walker. *Fundamentos de física 1: mecânica*. Livros Técnicos e Científicos Rio de Janeiro, 1996.

M. L. Jayaramu, H. Suresh, M. S. Bhaskar, D. Almakhles, S. Padmanaban, and U. Subramaniam. Real-time implementation of extended kalman filter observer with improved speed estimation for sensorless control. *IEEE Access*, 9: 50452–50465, 2021.

P. Krause, O. Wasynczuk, S. Sudhoff, and S. Pekarek. Analysis of electric machinery and drive systems, willey, 2013.

V. S. Madureira, T. P. das Chagas, and G. Q. de Jesus. Solar irradiance estimation using kalman filter. *Journal of Control, Automation and Electrical Systems*, 31(6):1447–1457, 2020.

J. Mamede Filho. *Instalações elétricas industriais*. Livros Tecnicos e Cientificos, 2007.

A. V. Oppenheim, A. S. Willsky, and S. H. Nawab. *Signals & Systems (2nd Ed.)*. Prentice-Hall, Inc., USA, 1996. ISBN 0138147574.

M. H. Rashid. Power electronics handbook-devices, circuits, and applications, 2011.

M. Stender, O. Wallscheid, and J. Bocker. Accurate torque estimation for induction motors by utilizing globally optimized flux observers. In *2020 International Symposium on Power Electronics, Electrical Drives, Automation and Motion (SPEEDAM)*, pages 219–226. IEEE, 2020.

E. Zerdali and M. Barut. Extended kalman filter based speed-sensorless load torque and inertia estimations with observability analysis for induction motors. *Power Electronics and Drives*, 3, 2018.

E. Zerdali and R. Demir. Speed-sensorless predictive torque controlled induction motor drive with feed-forward control of load torque for electric vehicle applications. *Turkish Journal of Electrical Engineering & Computer Sciences*, 29 (1):223–240, 2021.

8. RESPONSIBILITY NOTICE

The authors are solely responsible for the printed material included in this paper.